Daniela Nasteska, Norio Harada, Kazuyo Suzuki, Shunsuke Yamane, Akihiro Hamasaki, Erina Joo, Kanako Iwasaki, Kimitaka Shibue, Takanari Harada, and Nobuya Inagaki

Chronic Reduction of GIP Secretion Alleviates Obesity and Insulin Resistance Under High-Fat Diet Conditions

Diabetes 2014;63:2332–2343 | DOI: 10.2337/db13-1563

Gastric inhibitory polypeptide (GIP) exhibits potent insulinotropic effects on β-cells and anabolic effects on bone formation and fat accumulation. We explored the impact of reduced GIP levels in vivo on glucose homeostasis, bone formation, and fat accumulation in a novel GIP-GFP knock-in (KI) mouse. We generated GIP-GFP KI mice with a truncated *prepro-GIP* gene. The phenotype was assessed in heterozygous and homozygous states in mice on a control fat diet and a high-fat diet (HFD) in vivo and in vitro. Heterozygous GIP-GFP KI mice (GIP-reduced mice [$GIP^{gfp/+}$]) exhibited reduced GIP secretion; in the homozygous state (GIP-lacking mice [$GIP^{gfp/gfp}$]), GIP secretion was undetectable. When fed standard chow, $GIP^{gfp/+}$ and $GIP^{gfp/gfp}$ mice showed mild glucose intolerance with decreased insulin levels; bone volume was decreased in $GIP^{gfp/gfp}$ mice and preserved in $GIP^{gfp/+}$ mice. Under an HFD, glucose levels during an oral glucose tolerance test were similar in wild-type, $GIP^{gfp/+}$, and $GIP^{gfp/gfp}$ mice, while insulin secretion remained lower. $GIP^{gfp/+}$ and $GIP^{gfp/gfp}$ mice showed reduced obesity and reduced insulin resistance, accompanied by higher fat oxidation and energy expenditure. GIP-reduced mice demonstrate that partial reduction of GIP does not extensively alter glucose tolerance, but it alleviates obesity and lessens the degree of insulin resistance under HFD conditions, suggesting a potential therapeutic value.

Gastric inhibitory polypeptide (GIP) is a 42–amino acid polypeptide produced by enteroendocrine K cells, which are located mainly in the upper parts of the small intestine. Its main secretagogues are glucose and, even more intensely, fats that reach the intestinal lumen soon after food intake (1). Following secretion, the hormone exerts its effects through specific, G-protein–coupled receptors located mainly in the stomach, pancreas, central nervous system, bone, and adipose tissue (2,3). Apart from its role in the inhibition of gastric acid secretion (4), GIP exhibits potent glucose-dependent insulinotropic action (5,6), and, therefore, it is classified as an incretin (3). In addition to its insulinotropic effect, in the absence of which glucose intolerance develops (7), GIP stimulates islet growth (8) and proliferation of β-cells (9), and reduces β-cell apoptosis (10,11). Studies of GIP receptor (GIPR) knock-out (GIPRKO) mice (7) describe GIP as an obesity-promoting factor in high-fat diet (HFD) conditions, and show that deletion of GIPR signaling causes resistance to obesity (12) but leads to osteoporosis (13), revealing an important role of GIP in bone metabolism. However, in these studies, as well as in a model of GIPR antagonism (14), the reported changes were focused on disrupted or blocked GIPR signaling. The condition of reduced GIP secretion and how it affects the pancreatic and extrapancreatic effects of GIP remain unclear.

The aim of the current study is to explore the potential of reduced GIP levels in vivo, and to define the impact on glucose homeostasis, bone formation, and fat accumulation in a novel GIP–green fluorescent protein (GFP) knock-in (KI) mouse model characterized by truncation of the *prepro-GIP* gene and insertion of a GFP sequence (15). The model was developed for the purpose of visualization and identification of K cells and exhibits reduced

Department of Diabetes, Endocrinology and Nutrition, Graduate School of Medicine, Kyoto University, Kyoto, Japan

Corresponding author: Nobuya Inagaki, inagaki@metab.kuhp.kyoto-u.ac.jp.

Received 11 October 2013 and accepted 25 February 2014.

This article contains Supplementary Data online at http://diabetes.diabetesjournals.org/lookup/suppl/doi:10.2337/db13-1563/-/DC1.

or absent GIP secretion in heterozygous GIP-reduced mice and homozygous or GIP-lacking mice, respectively. Establishing the phenotype of the heterozygous GIP-reduced mouse is important to understand the possible benefits of a limited reduction of GIP secretion.

RESEARCH DESIGN AND METHODS

Animals

Male GIP-GFP KI mice and wild-type (WT) littermates were used in all experiments. GIP-GFP KI mice were generated as described previously (15). The animals were maintained under conditions of a 12 h light/dark cycle, with free access to water and food, unless indicated otherwise. Starting from 7 weeks of age, the mice were divided into the following two groups: the control fat diet (CFD) group, receiving food with 10% of fat and energy density of 3.8 kcal/g (catalog no. D12450B; Research Diets Inc., New Brunswick, NJ); and the HFD group, receiving food with 60% of fat and energy density of 5.2 kcal/g (catalog no. D12492; Research Diets Inc.). In total, six groups of mice (five to six mice per group) were used throughout the study: WT mice on CFD, heterozygous GIP-GFP KI mice ($GIP^{gfp/+}$) on CFD, homozygous GIP-GFP KI mice ($GIP^{gfp/gfp}$) on CFD, WT on HFD, $GIP^{gfp/+}$ mice on HFD, and $GIP^{gfp/gfp}$ on HFD. After 8 weeks of CFD or HFD feeding, the animals were used in the experiments listed below. Maintenance of the mice and all experimental procedures were approved by Kyoto University Animal Care Committee.

Expression Levels of GIPR mRNA

After standard chow feeding or at least 8 weeks of CFD and HFD feeding, mice were killed by cervical dislocation, and the pancreas and white (visceral) adipose tissue were harvested. The white adipose tissue was frozen immediately in liquid nitrogen and stored at −80°C until further use; the pancreas was digested using the collagenase method, and islets were obtained. Islet mRNA (RNeasy Mini Kit; Qiagen, Hilden, Germany) and adipose tissue mRNA (RNeasy Lipid Tissue Mini Kit; Qiagen) were extracted and cDNA was synthesized by reverse transcription (SuperScript II; Invitrogen, Carlsbad, CA). GIPR mRNA expression levels were quantified by semiquantitative real-time PCR (AB StepOne Plus Real Time PCR; Applied Biosystems, Foster City, CA) using GIPR forward and reverse primers with the following sequence: 5′-CCTCCACTGGGTCCCTACAC-3′ (forward primer) and 5′-GATAAACACCCTCCACCAGTAG-3′ (reverse primer). Glyceraldehyde-3-phosphate dehydrogenase (GAPDH) mRNA was used as an internal control. The sequences of GAPDH forward and reverse primers are as follows: 5′-AAATGGTGAAGGTCGGTGTG-3′ for the forward primer, and 5′-TCGTTGATGGCAACAATCTC-3′ for the reverse primer.

Measurement of GIP Content and Protein Content

Mice were killed at 6 weeks of age by cervical dislocation, intestine samples were taken and washed in PBS, weighed, and, after overnight extraction with 5 mL/g acid ethanol (at 4°C), GIP content was measured by ELISA (Millipore Corp., Billerica, MA). Protein content was measured using Bradford Protein Assay (Bio-Rad, Hercules, CA). In brief, dye reagent was diluted, and protein (albumin) standards were made in duplicate. Standards and intestine samples were loaded on a microtiter plate, incubated at room temperature for 5 min, and absorbance was measured at 595 nm. GIP content was expressed as GIP content per protein content.

Bone Histomorphometry

Six-week-old mice that had been fed standard chow were prepared for bone histomorphometry measurement by subcutaneous injection of 25 mg/kg tetracycline hydrochloride (Sigma-Aldrich, St. Louis, MO) 4 days before they were killed and 10 mg/kg calcein (Dojindo, Kumamoto, Japan) 2 days before they were killed. Animals were killed by cervical dislocation, and tibiae were removed and fixed with 70% ethanol. Further processing of tibiae samples (muscle removing, dehydration in graded concentration of ethanol, Villanueva bone staining, and embedding in methyl methacrylate), preparation of frontal plane sections of tibiae, and bone histomorphometry measurement using a semiautomatic image-analyzing system (System Supply, Nagano, Japan) were performed by Niigata Bone Science Institute, Niigata, Japan.

Oral Glucose Tolerance Test and Measurement of Hormones

Following 8 weeks of CFD and HFD, the mice underwent an oral glucose tolerance test (OGTT). The fasting period (overnight fasting) was begun 19 h prior to the experiment. During the test, blood samples were obtained by heparinized microcapillary tubes from the orbital sinus of the mice at the following time intervals: 0 min (fasting levels), and 15, 30, 60, and 120 min after glucose administration. Glucose (2 g/kg in mice on standard chow and 1 g/kg in mice on HFD) was given orally, using a gavage tube. Blood glucose levels were measured by the glucose oxidase method (Sanwa Kagaku Kenkyusho, Nagoya, Japan). After collection, blood samples were kept on ice and then centrifuged (3,000 rotations per minute for 10 min at 4°C), and serum was separated. The serum samples were used fresh or kept at −80°C until further processing. Insulin, total GIP, and total glucagon-like peptide 1 (GLP-1) levels were measured by ELISA as follows: insulin kit (Shibayagi, Shibukawa, Japan), total GIP kit (Millipore, Billerica, MA), and total GLP-1 kit (Meso Scale Discovery, Rockville, MD).

Insulin Tolerance Test

The mice were fasted 4–6 h before the start of the experiment. Blood samples were drawn from the orbital sinus using heparinized microcapillary tubes at the following time intervals: 0 min (fasting levels), and 15, 30, 60, and 120 min after insulin administration. Human insulin (100 units/mL; Eli Lilly and Co., Indianapolis, IN) was

administered intraperitoneally in a dose of 0.5 units/kg. Blood glucose levels were measured by the glucose oxidase method (Sanwa Kagaku Kenkyusho).

Measurement of Body Fat Composition (Measurement of Subcutaneous and Visceral Fat)

In young mice at the age of 7 weeks, or after 8 weeks of feeding with a CFD or HFD, body fat was measured by a computed tomography (CT) scan (A La Theta LCT-100; Hitachi Aloka, Tokyo, Japan). The mice were anesthetized with intraperitoneal injection of sodium pentobarbital and placed in a measurement chamber of the CT scanner in the supine position. The scanned area of the body was flanked by the xiphisternum and sacrum; the width of scanned slices was 2 mm. The images obtained were analyzed using A La Theta software, version 1.00, and values for body fat, both subcutaneous and visceral, were quantified in grams.

Indirect Calorimetry and Mice Activity

Mice were kept 6–7 weeks on CFD or HFD, and afterward indirect calorimetry was performed and the activity of the mice was measured (ARCO 2000 mass spectrometer; Arco System, Chiba, Japan). Each mouse was placed in an individual chamber with free access to water and CFD or HFD. Respiratory quotient, energy expenditure (in calories per minute per kilogram), fat oxidation (in milligrams per minute per kilogram), and mice activity (in counts per minute) were measured every 5 min over 48 h.

In Vitro Insulin Secretion

For the measurement of glucose-stimulated insulin secretion in vitro, islets from mice on CFD and HFD were isolated using collagenase digestion method. In brief, mice were killed by cervical dislocation; 0.5 mg/mL collagenase dissolved in Hanks' balanced salt solution was injected through the bile duct into the pancreas, and, after its expansion, it was manually isolated and incubated in Krebs-Ringer bicarbonate buffer (KRBB; 120 mmol/L NaCl, 4.7 mmol/L KCl, 1.2 mmol/L $MgSO_4$, 1.2 mmol/L KH_2PO_4, 2.4 mmol/L $CaCl_2$, and 20 mmol/L $NaHCO_3$) at 37°C over 21 min. After homogenizing the pancreas with KRBB, the islets were separated by centrifugation in Ficoll gradient. Separated islets were resuspended in KRBB on a dish and handpicked under a light microscope. For glucose-stimulated insulin secretion assessment, three batches with different glucose concentrations were prepared, as follows: 5.5 mmol/L glucose, 11.1 mmol/L glucose, and 11.1 mmol/L glucose plus 100 nmol/L GIP-human (Peptide Institute, Osaka, Japan). For each sample containing 500 μL incubation medium (KRBB; 2 mol/L HEPES, pH 7.4; 0.2% BSA), 10 islets were handpicked in a volume of 200 μL KRBB and incubated at 37°C during 30 min (following preincubation in the same conditions). For the measurement of insulin content in islets of HFD-fed mice, samples were incubated overnight with 5 mL/g acid ethanol (at 4°C). Insulin concentration and insulin content were measured using radioimmunoassay (Aloka Accuflex γ 7000; Hitachi, Tokyo, Japan).

Measurement of β-Cell Area

Whole pancreas was isolated manually from mice kept on CFD and HFD for 8 weeks. All isolated organs were fixed in Bouin's solution, then were washed with 50% ethanol once per day over 1 week, and, finally, embedded in paraffin. Every fifth section of the pancreas was used for analysis. In total, three sections (slides) per pancreas (per mouse) were analyzed. The paraffin slides were deparaffinized with lemosol, rehydrated with 100% and 70% ethanol, blocked by 3% peroxidase, incubated overnight (at 4°C) in a humidified chamber with polyclonal rabbit anti-insulin antibody (Santa Cruz Biotechnology, Santa Cruz, CA), and conjugated with fluorescent secondary antibody the next day. After immunostaining, all slides were analyzed by immunofluorescent microscope (Keyence Corp., Osaka, Japan) using BZ Analyzer software. The area of the whole pancreas and the area of insulin-immunopositive cells were measured at the same time. The β-cell area was expressed as β-cell area/total pancreas area in all analyzed slides.

Statistics

All results are expressed as the mean ± SE. Statistical analyses were performed using ANOVA with Tukey test, and P values <0.05 were considered statistically significant.

RESULTS

GIP Reduction in GIP-GFP KI Mice

The main genetic trait of GIP-GFP KI mice is alteration (truncation) of the *prepro-GIP* gene coupled with insertion of the GFP coding sequence (15). In mice kept on standard chow, the assessment of GIP mRNA levels in the small intestine showed reduced levels in $GIP^{gfp/+}$ mice ($P < 0.05$), while in $GIP^{gfp/gfp}$ mice, GIP mRNA could not be detected ($P < 0.05$, $P < 0.01$) (Fig. 1*A*). Small intestine GIP contents were reduced in $GIP^{gfp/+}$ mice ($P < 0.05$) and were undetectable in $GIP^{gfp/gfp}$ mice ($P < 0.01$) when compared with WT mice. Total GIP levels during OGTT (Fig. 1*B*) as well as GIP secretion (as shown by the area under the curve of GIP) (Fig. 1*C*) were reduced by ~50% in $GIP^{gfp/+}$ mice ($P < 0.01$) and were below the lower limit of detection in $GIP^{gfp/gfp}$ mice ($P < 0.001$) compared with control WT mice (the lower detection limit of ELISA total GIP levels kit was 8.2 pg/mL).

Body Weight Progression, Glucose Tolerance, and β-Cell Profile Following GIP Reduction in Standard Chow-Fed Mice

Starting from 4 weeks of age, the body weight of weaning mice fed standard chow (containing 10% fat) was recorded, and no changes were seen among WT, $GIP^{gfp/+}$, and $GIP^{gfp/gfp}$ mice (Fig. 2*A*). The measurement of body fat composition (body fat) in the 7th week of age (just before placing the mice on an HFD) revealed similar amounts of body fat in all mice (Fig. 2*B*). During an OGTT, blood glucose levels were higher in $GIP^{gfp/+}$ mice than those in WT mice at 30 min ($P < 0.05$), whereas in $GIP^{gfp/gfp}$

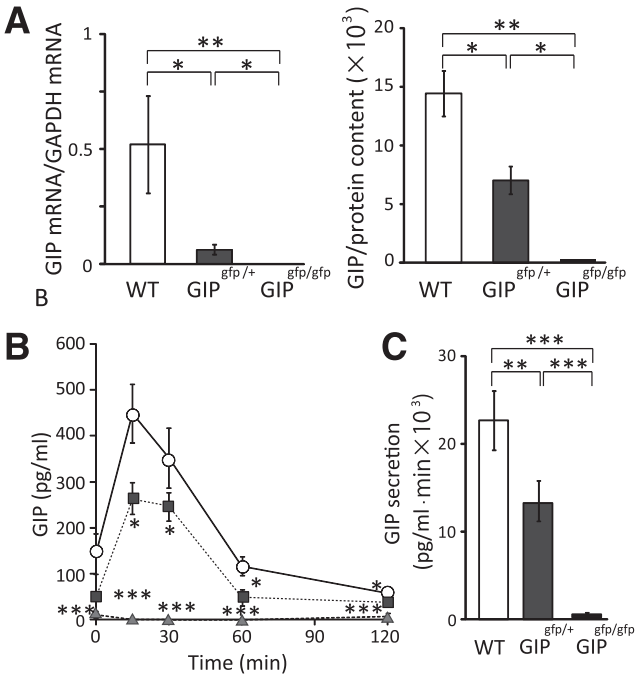

Figure 1—GIP reduction in GIP-GFP KI mice. *A*: The following measurements were conducted in the small intestine of WT, $GIP^{gfp/+}$, and $GIP^{gfp/gfp}$ mice: assessment of GIP mRNA levels (expressed as GIPR mRNA/GAPDH mRNA) and GIP content (expressed as GIP/protein content). Total GIP levels (*B*) and GIP secretion (the area under the curve of GIP) (*C*) were measured during the OGTT (glucose 2 g/kg body weight). $n = 5–6$ per group. WT mice are represented by white bars and white circles, $GIP^{gfp/+}$ mice are represented by black bars and black squares, and $GIP^{gfp/gfp}$ mice are represented by gray bars and gray triangles. $^*P < 0.05$, $^{**}P < 0.01$, $^{***}P < 0.001$.

mice glucose elevation persisted at 30 and 60 min ($P < 0.05$) (Fig. 2*C*). Meanwhile, insulin levels in both $GIP^{gfp/+}$ and $GIP^{gfp/gfp}$ remained lower in comparison with WT, especially at 15 and 30 min after glucose load ($P < 0.05$) (Fig. 2*D*). In vitro measurement of insulin secretion (Fig. 2*E*) showed a similar pattern of secretion in all types of mice at 5.5 mmol/L glucose, as well as at 11.1 mmol/L glucose. When challenged with 100 nmol/L human GIP peptide together with 11.1 mmol/L glucose, the islets of GIP-GFP KI mice, both $GIP^{gfp/+}$ and $GIP^{gfp/gfp}$, exhibited a similar insulin response to that of WT mice. GIPR mRNA levels in β-cells remained unchanged in GIP-GFP KI mice when compared with controls (Fig. 2*F*). mRNA expression of preproglucagon, peptide YY, cholecystokinin, somatostatin, and secretin in the small intestine showed no differences in GIP-GFP KI mice compared with WT mice (data not shown). Plasma GLP-1 levels during the OGTT did not differ among the three types of mice (WT mice 15.54 ± 6.8 pg/mL, $GIP^{gfp/+}$ mice 11.83 ± 4.97 pg/mL, $GIP^{gfp/gfp}$ mice 18.54 ± 3.96 pg/mL at 15 min after OGTT).

Body weight follow-up of mice on CFD in a period of 8 weeks (starting at the age of 7 weeks) showed that the body weight progression did not differ among all three groups of mice (Supplementary Fig. 1*A*). The overall glucose response to 0.5 units/kg human insulin (insulin tolerance test [ITT] data) was similar in WT, $GIP^{gfp/+}$, and $GIP^{gfp/gfp}$ mice at almost all time points of the experiment (at 60 min of ITT, $GIP^{gfp/gfp}$ mice had lower blood glucose levels when compared with WT mice) (Supplementary Fig. 1*B*).

Bone Formation in Conditions of Standard Chow Feeding

Following GIP reduction, the bone volume in $GIP^{gfp/+}$ mice was similar to that in WT mice, whereas $GIP^{gfp/gfp}$ mice had reduced bone volume ($P < 0.05$) (Fig. 3*A*). Furthermore, the number of trabeculae in $GIP^{gfp/+}$ mice showed no changes when compared with WT mice, while $GIP^{gfp/gfp}$ mice exhibited a decrease ($P < 0.05$) (Fig. 3*C*), as demonstrated by the images of proximal tibial sections (Fig. 3*B*). Although osteoblast surface was decreased in $GIP^{gfp/+}$ mice compared with WT mice ($P < 0.05$) (Fig. 3*D*), the bone formation rate (Fig. 3*F*) remained unchanged in these mice. The osteoclast surface was increased in $GIP^{gfp/gfp}$ mice ($P < 0.05$) when compared with WT mice, while in $GIP^{gfp/+}$ mice it remained similar to WT mice (Fig. 3*E*).

Induction of Metabolic Stress by HFD

Figures 4 and 5 describe the phenotype changes induced by HFD feeding for 8 weeks (56 days). Starting from the second week of HFD feeding, WT mice steadily increased their body weight ($P < 0.001$) compared with the lean control (Fig. 4*A*), while within the HFD group, $GIP^{gfp/+}$ mice showed less body weight gain ($P < 0.01$ at 2nd week; $P < 0.001$ at 8th week) than WT mice; $GIP^{gfp/gfp}$ mice exhibited the lowest body weight gain ($P < 0.001$ at 2nd week; $P < 0.001$ at 8th week vs. WT HFD). Ad libitum glucose levels were measured at the same time, once per week, and the overall glucose levels in all mice remained similar (Fig. 4*B*). Food and water intake were similar in all groups of mice (data not shown).

During OGTT, total GIP levels and GIP secretion were increased twofold in WT mice on HFD ($P < 0.001$) compared with the lean control; in HFD-fed mice, $GIP^{gfp/+}$ mice exhibited decreased levels ($P < 0.05$), while $GIP^{gfp/gfp}$ mice showed an absence of GIP ($P < 0.001$) (Fig. 4*C* and *D*). Fasting glucose levels in WT mice on HFD were higher ($P < 0.01$) when compared with their lean littermates; on HFD background, glucose levels remained similar in all mice (Fig. 4*E*). The overall insulin response (Fig. 4*F*) in WT mice on HFD was more intense than that of the control mice, and, within the HFD group, the insulin levels of $GIP^{gfp/+}$ mice remained lower in comparison with those of WT mice ($P < 0.05$), while $GIP^{gfp/gfp}$ mice showed the lowest insulin levels ($P < 0.01$, $P < 0.001$). Insulin secretion in vitro (Fig. 4*G*) was similar among all mice on CFD and HFD in the presence of 5.5 mmol/L glucose. In response to 11.1 mmol/L glucose, WT mice on HFD had higher insulin secretion compared with WT mice on CFD, whereas in the HFD group similar levels were found in WT and $GIP^{gfp/+}$ mice, coupled with lower

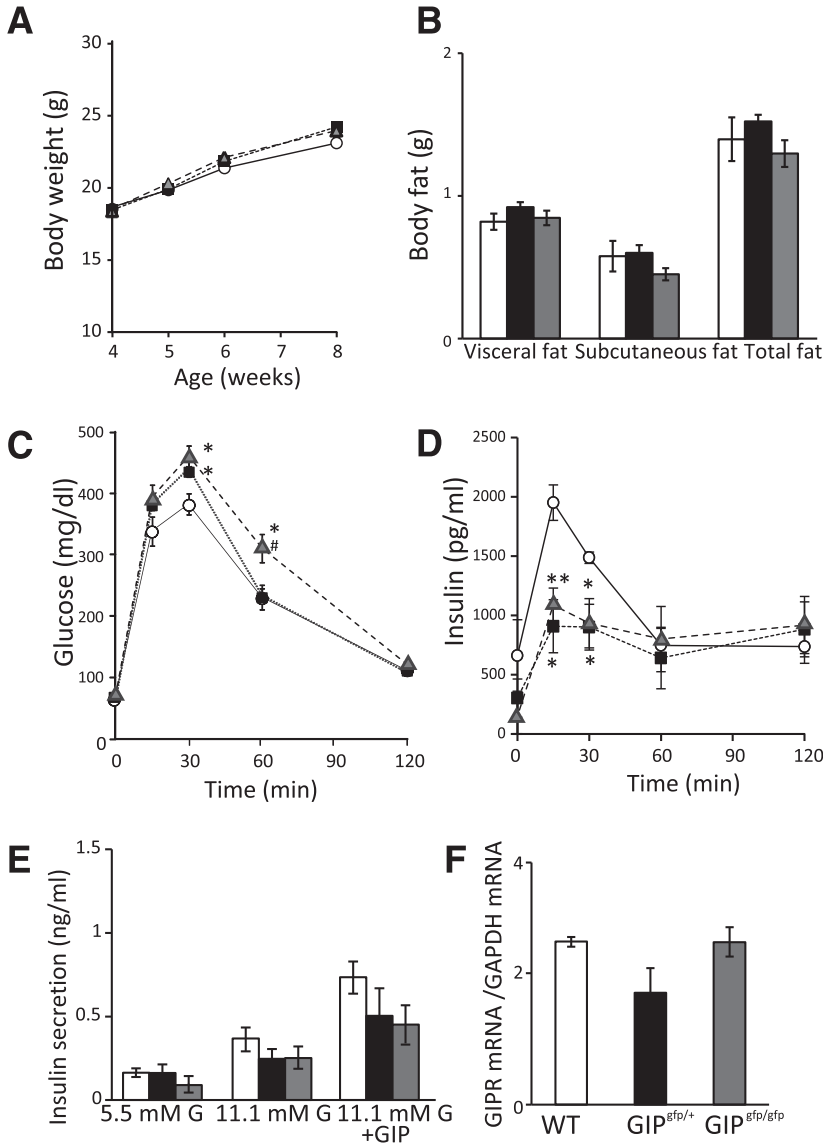

Figure 2—Body weight, glucose tolerance, and β-cell profile following GIP reduction in standard chow-fed mice. *A*: Body weight of weaning mice (4 weeks old) was measured starting from the beginning of the weaning period until the age of 8 weeks (body weight in the 7th week of age was not measured because of CT scan measurement and postanesthesia recovery period). *B*: Body fat was measured by CT scan in the 7th week of age. Glucose (*C*) and insulin (*D*) levels were measured during OGTT (glucose load of 2 g/kg body weight). *E*: In vitro insulin secretion from isolated islets was measured in conditions of 5.5 mmol/L glucose, 11.1 mmol/L glucose, and 11.1 mmol/L glucose plus 100 nmol/L human GIP. *F*: GIPR mRNA levels in islets were expressed as GIPR mRNA/GAPDH mRNA. n = 5–6 mice or samples per group; 10 islets per sample. WT mice are represented by white circles and white bars, $GIP^{gfp/+}$ mice are represented by black squares and black bars, and $GIP^{gfp/gfp}$ mice are represented by gray triangles and gray bars. *$P < 0.05$, **$P < 0.01$ vs. WT; #$P < 0.05$ vs. $GIP^{gfp/+}$ mice.

insulin levels in $GIP^{gfp/gfp}$ mice ($P < 0.05$ vs. WT HFD, $P < 0.01$ vs. $GIP^{gfp/+}$). When 100 nmol/L human GIP peptide was added to 11.1 mmol/L glucose, insulin secretion remained lower in $GIP^{gfp/gfp}$ mice on HFD ($P < 0.01$). Measurement of the β-cell area, as expressed by the ratio of β-cell area to total pancreas area, showed a tendency toward an increase observed in HFD-fed mice, relative to the lean mice, although the difference was not statistically significant. However, within the HFD group, β-cell area remained similar in WT and $GIP^{gfp/+}$ mice, while $GIP^{gfp/gfp}$ mice exhibited decreased β-cell area ($P < 0.05$) (Fig. 4*H*). The expression levels of GIPR mRNA in the islets were similar in WT mice on CFD and HFD, as well as in $GIP^{gfp/+}$ mice on HFD, whereas in $GIP^{gfp/gfp}$ mice levels were reduced ($P < 0.01$ vs. $GIP^{gfp/+}$) (Fig. 4*I*).

Adipose Tissue Response to HFD Feeding and Consequential Energy Expenditure Changes

CT scan measurement (Fig. 5*A*) of visceral, subcutaneous, and total body fat demonstrated a large increase in fat accumulation in WT mice on HFD ($P < 0.01$) when compared with the lean mice. On an HFD background, WT

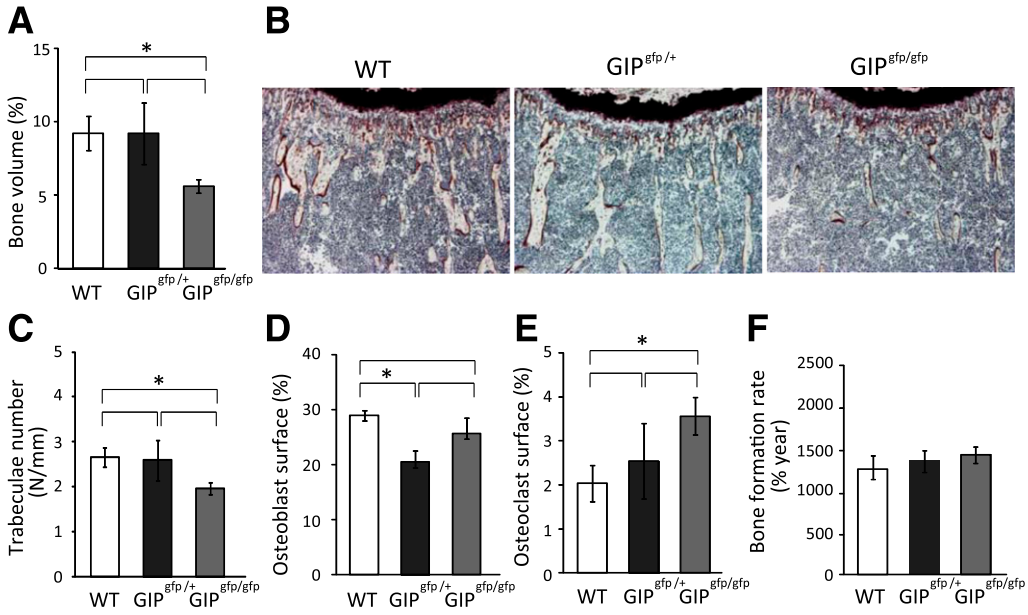

Figure 3—Bone formation in conditions of standard chow feeding. The following parameters were measured by bone histomorphometry: bone volume (expressed as bone volume %) (*A*), trabeculae number (expressed as number per millimeter) (*C*), osteoblast surface (%) (*D*), osteoclast surface (%) (*E*), and bone formation rate (%/year) (*F*). *B*: Images display trabeculae of proximal tibial sections taken from 6-week-old mice. n = 5–6 per group. WT mice are represented by white bars, $GIP^{gfp/+}$ mice are represented by black bars, and $GIP^{gfp/gfp}$ mice are represented by gray bars. *$P < 0.05$ vs. WT mice. The absence of an asterisk above the horizontal brackets in *A* and *C–E* indicates no statistical significance.

mice accumulated more body fat than their $GIP^{gfp/+}$ littermates ($P < 0.05$), while the fat depots in $GIP^{gfp/gfp}$ were greatly reduced ($P < 0.01$), showing levels similar to the lean control. The CT scan images of abdominal sections of mice on CFD and HFD visualize the difference in fat accumulation among all groups. Assessment of insulin resistance by ITT (Fig. 5*B*) showed a rise in glucose levels in HFD-fed WT mice compared with lean mice, while within the HFD group a better response to insulin was observed in both $GIP^{gfp/+}$ and $GIP^{gfp/gfp}$ mice, with glucose levels remaining lower ($P < 0.05$; $P < 0.01$) compared with WT mice. In relation to these data, a tendency toward increased fat oxidation (Fig. 5*C*) in all mice on HFD was observed ($P < 0.05$), with a larger increase in $GIP^{gfp/+}$ mice ($P < 0.05$), especially in the dark phase, and even higher in $GIP^{gfp/gfp}$ mice ($P < 0.05$). In addition, the energy expenditure measurement on HFD background (Fig. 5*D*) showed an increase in $GIP^{gfp/+}$ mice ($P < 0.05$) (again, more prominent in the dark phase) and in $GIP^{gfp/gfp}$ mice ($P < 0.05$) when compared with WT mice. Concomitantly, mice activity was measured (Fig. 5*E*), and no statistically significant changes were found in the HFD group. Expression levels of GIPR mRNA in white (visceral) adipose tissue (Fig. 5*F*) remained unchanged in all animals on CFD and HFD, except for $GIP^{gfp/gfp}$ mice, in which the levels were elevated ($P < 0.05$).

DISCUSSION

Studies in single and double incretin receptor knock-out mice (16) have shown that, although secretion of GIP and GLP-1 is triggered by different factors, they have an additive stimulating effect on β-cells with regard to insulin secretion, with GIP accounting for the larger portion of the total incretin effect in male mice. Furthermore, human data demonstrated that after an oral glucose load of 75 g and a mixed meal load (17,18), secretion of GIP is more pronounced than GLP-1 secretion, suggesting that GIP may play a more potent role in the regulation of postprandial insulin secretion in nondiabetic conditions. We have generated GIP-GFP KI mice characterized by truncation of the *prepro-GIP* gene and insertion of the GFP coding sequence that leads to reduced GIP production in heterozygous state and the absence of GIP production in the homozygous state. $GIP^{gfp/gfp}$ mice exhibit a phenotype similar to that of GIPRKO mice regarding glucose tolerance, bone formation, and adipose tissue expansion (Table 1). However, $GIP^{gfp/+}$ mice represent a novel mouse model in which GIP, despite its secretion being reduced by half, maintains glucose levels similar to those of controls (Fig. 4*B* and *E*) and lessens insulin resistance in mice with HFD-induced obesity (Figs. 4*F* and 5*B*).

When fed standard chow, $GIP^{gfp/gfp}$ mice, in a manner similar to GIPRKO mice, had higher glucose excursions accompanied with insufficient production of insulin during OGTT (Table 1). Despite having reduced, but still present, GIP secretion, $GIP^{gfp/+}$ mice also showed mild glucose intolerance and lower insulin secretion, confirming the potent insulinotropic effect of GIP (Fig. 2*C* and *D*, and Table 1). Furthermore, insulin secretion tests in vitro

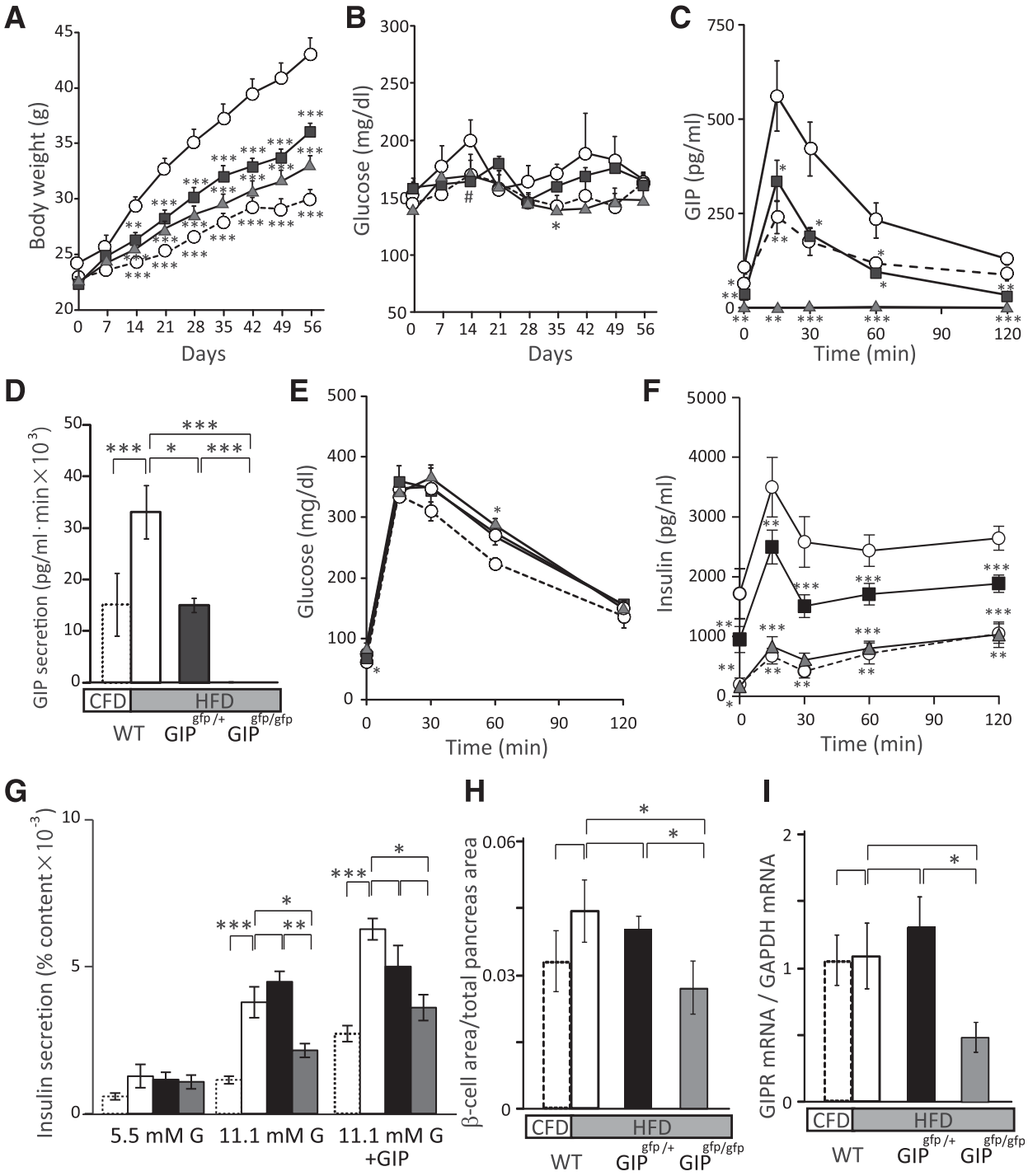

Figure 4— Induction of metabolic stress by HFD. Body weight (*A*) and ad libitum glucose levels (*B*) in WT CFD, WT HFD, GIP$^{gfp/+}$ HFD, and GIP$^{gfp/gfp}$ HFD mice were measured once per week during 8 weeks (56 days) of feeding with CFD (10% of fat) or HFD (60% of fat). Total GIP levels (*C*), GIP secretion (GIP area under the curve) (*D*), glucose levels (*E*), and insulin levels (*F*) were measured during OGTT (glucose load of 1 g/kg body weight) conducted after 8 weeks (56 days) of CFD or HFD feeding. *G*: In vitro insulin secretion from isolated islets was measured in conditions of 5.5 mmol/L glucose, 11.1 mmol/L glucose, and 11.1 mmol/L glucose plus 100 nmol/L human GIP. Results were expressed as insulin secretion (% insulin content). *H*: β-Cell area was measured by immunohistochemistry of pancreas sections and subsequent analysis using BZ Analyzer software. Results are expressed as β-cell area/total pancreas area. *I*: GIPR mRNA levels in islets were expressed as GIPR mRNA/GAPDH mRNA. n = 5–6 mice or samples per group; 10 islets per sample. WT CFD mice are represented by white circles with square dot dash and white bars with square dot border, WT HFD mice are represented by white circles with solid dash and white bars with solid border, GIP$^{gfp/+}$ mice are represented by black squares and black bars, and GIP$^{gfp/gfp}$ mice are represented by gray triangles and gray bars. P values are expressed as follows: *A*, *C*–*F*: *P < 0.05, **P < 0.01, ***P < 0.001 vs. WT HFD; *B*: *P < 0.05 WT CFD vs. WT HFD; and #P < 0.05 GIP$^{gfp/+}$ HFD vs. WT HFD; *G*–*I*: *P < 0.05, **P < 0.01, ***P < 0.001. The absence of an asterisk above the horizontal brackets in *G*–*I* indicates no statistical significance.

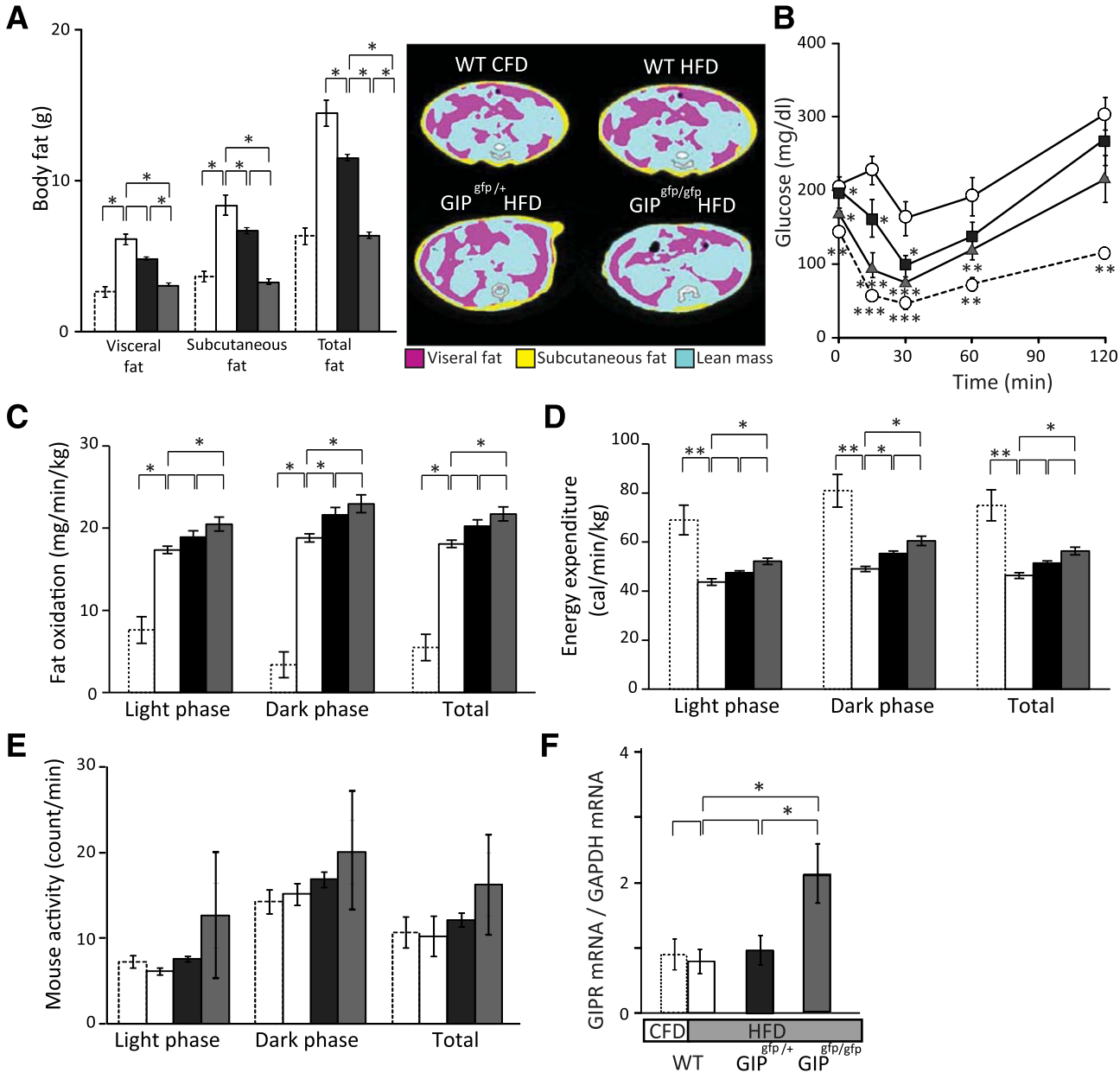

Figure 5—Adipose tissue response to HFD feeding and consequential energy expenditure changes. *A*: Visceral, subcutaneous, and total fat (expressed in grams) in WT CFD, WT HFD, GIP$^{gfp/+}$HFD, and GIP$^{gfp/gfp}$ HFD mice were measured, and CT images of transverse abdominal sections were taken after 8 weeks of feeding with CFD (10% of fat) or HFD (60% of fat). *B*: ITT (insulin 0.5 units/kg of body weight) was conducted after 8 weeks of CFD or HFD. Fat oxidation (in milligrams per minute per kilogram) (*C*), energy expenditure (calories per minute per kilogram) (*D*), and mice activity (counts per minute) (*E*) were measured after 6–7 weeks of CFD or HFD. *F*: GIPR mRNA levels in white (visceral) adipose tissue were expressed as GIPR mRNA/GAPDH mRNA. n = 5–6 mice or samples per group. WT CFD mice are represented by white bars with square dot border and white circles with square dot dash; WT HFD mice are represented by white bars with solid border and white circles with solid dash; GIP$^{gfp/+}$ HFD mice are represented by black bars and black squares; and GIP$^{gfp/gfp}$ HFD mice are represented by gray bars and gray triangles. *P* values are expressed as follows: *B*: $^{*}P < 0.05$, $^{**}P < 0.01$, $^{***}P < 0.001$ vs. WT HFD; *A*, *C*, *D*, and *F*: $^{*}P < 0.05$, $^{**}P < 0.01$. The absence of an asterisk above the horizontal brackets in *A*, *C*, *D*, and *F* indicates no statistical significance.

demonstrated a similar pattern of secretion in all groups of mice. The measurement of mRNA expression levels of GIPR in the islets showed no changes among all groups of mice, indicating the presence of functional GIPRs.

Similar to GIP-lacking and GIP-reduced mice, rat GIP promoter-diphtheria toxin A chain transgenic mice exhibit glucose intolerance, in their case very profound, with complete abolition of the incretin effect, and show similarities in phenotype under HFD conditions (19). In this mouse model (GIP promoter-diphtheria toxin A chain), forced expression of attenuated diphtheria toxin was established under the rat GIP promoter, leading to isolated

Table 1—Phenotype comparison of GIP-GFP KI mice and GIPRKO mice

Genotype/phenotype	$GIP^{gfp/+}$	$GIP^{gfp/+}$ HFD	$GIP^{gfp/gfp}$	$GIP^{gfp/gfp}$ HFD	GIPRKO (7,13)	GIPRKO HFD (6,12,29)
Standard chow feeding						
GIP secretion	↓ (~50%)		Absent		↑	
Glucose tolerance	Impaired		Impaired		Impaired	
Bone volume	↔		↓		↓	
HFD feeding						
Glucose tolerance		↔		↔		Impaired
Body weight		↓		↓↓		↓↓
Fat mass		↓		↓↓		↓↓
Insulin sensitivity		↑		↑↑		↑↑

Standard chow feeding data are relative to WT; HFD feeding data are relative to WT HFD. ↔, no changes; ↓, decreased; ↓↓, highly decreased; ↑, increased; ↑↑, highly increased.

ablation of GIP-producing cells, and, subsequently, the absence of GIP mRNA transcripts and absence of circulating GIP levels. However, there are reports confirming the existence of double incretin-positive cells (K/L cells) in the intestine (20), and the existence of populations of K cells that coexpress not only GIP but also glucagon, somatostatin, secretin, and, to a smaller extent, some other hormones (21,22). Therefore, the ablation of K cells might affect the number and/or distribution of these cell populations and could influence the accurate assessment of secretion of various intestinal hormones. In the case of GIP-GFP KI mice, the truncation of the *prepro-GIP* gene and expression of GIP-GFP fusion protein were driven by native GIP promoter, enabling selective changes in K cells that affect only GIP secretion and, even more importantly, control of the levels of GIP production. The expression levels of mRNA of the intestinal hormones preproglucagon, peptide YY, cholecystokinin, somatostatin, and secretin were not changed, confirming that GIP reduction did not interfere with their gene expression.

There are reports demonstrating that GIP induces GLP-1 secretion (23,24). Previously conducted studies of disrupted or blocked GIPR signaling (7,16,19) did not yield data regarding the secretion of GLP-1. In our study, plasma GLP-1 levels remained unchanged in GIP-GFP KI mice, as reported earlier in a model of GIPR antagonism (14), indicating that the reduction of GIP secretion does not affect GLP-1 secretion. Overall, GIP-reduced mice kept on standard chow after birth did not exhibit visible abnormalities regarding mating potential, pregnancy, offspring viability, growth, organ composition, and feeding behavior (data not shown). Measurement of their body weight from the beginning of the weaning period (Fig. 2*A*) until just before the shift to HFD, as well as longer-term measurement (Supplementary Fig. 1*A*), showed that they are not different from their WT littermates when fed a standard diet. Body fat measured before the start of the HFD was similar between WT and GIP-GFP KI mice. ITT showed that their insulin sensitivity remained similar to the WT mice (Supplementary Fig. 1*B*).

In addition to its insulinotropic role, GIP is involved in modulation of bone formation. There are GIP-specific receptors located on osteoblasts (25) and osteoclasts (26). GIP operates as an anabolic hormone in the bone, where it stimulates incorporation of meal-derived Ca^{2+} into bone and bone building (13), and reduces bone absorption by inhibiting osteoclastic activity. Studies in GIPRKO mice have shown that the absence of GIPR signaling leads to significant osteoporosis due to lower osteoblast and higher osteoclast action (13). Similar to GIPRKO mice, GIP-lacking mice also showed signs of osteoporosis, manifested by reduced bone volume, reduced number of trabeculae, and increased osteoclast surface. On the other hand, GIP-reduced mice maintained normal bone volume and bone trabeculae, and, despite the exhibited reduction of osteoblast surface, no increased osteoclast activity was observed. More importantly, the bone formation rate remained normal, indicating that reduction of GIP by ~50% does not significantly impair the beneficial role of GIP in bone formation. Considering the glucose intolerance of these mice, it appears that reduction of GIP secretion more profoundly affects the insulin-potentiating role of GIP, indicating differing regulatory mechanisms of GIP action in β-cells and in bone (Table 1).

To better understand the extent of the phenotypic consequences following GIP reduction, we induced chronic metabolic stress by feeding the mice with HFD. Previous reports indicate a strong connection between GIP secretion and obesity in HFD-feeding conditions (27). High caloric intake causes hypersecretion of GIP (12,28,29) due to hyperexpression of the GIP gene (15) and a subsequent rise in insulin secretion (30), leading to increased fat deposition in the adipose tissue and expansion of fat depots (31,32). GIP increases the adipose tissue volume directly (33,34) by binding to its receptors located on the adipocytes and indirectly by potentiating β-cell secretion of insulin, which is known to be involved in adipocyte fat deposition (35). In our study, HFD feeding for at least 8 weeks resulted in the absence of circulating GIP levels in GIP-lacking mice (consistent with data from standard chow-fed mice), whereas in GIP-reduced

mice, the reduction of GIP was similar to the levels observed in lean WT mice and was lower when compared with WT mice on HFD. The most obvious consequence of HFD was a change in body weight and fat mass in WT and GIP-GFP KI mice (Figs. 4*A* and 5*A*, and Table 1). Although WT mice showed overt obesity, GIP-lacking mice retained their body weight and fat mass at levels similar to those of their lean littermates, as previously reported in GIPRKO mice, in mice with K-cell ablation (19) and in mice with chemical inhibition of GIPR signaling (14). GIP-reduced mice also maintained lower body weight throughout the experiment period of 56 days, indicating that while the lack of body weight gain and fat mass was not as evident as it was in GIP-lacking mice, the reduced obesity was nevertheless important. Moreover, the glucose response to insulin during ITT showed lower levels in both GIP-reduced and GIP-lacking mice fed HFD, indicating that not only complete but also partial reduction of GIP alleviates insulin resistance while reducing obesity. Thus, a reduction of GIP secretion as shown in GIP-reduced mice mitigates both direct and indirect actions of GIP on adipose tissue and leads to reduced diet-induced obesity.

Glucose levels measured ad libitum throughout most of the experiment period were similar in WT mice and GIP-GFP KI mice, and glucose excursions during OGTT remained similar as well in all mice under HFD conditions. However, all HFD-fed mice had higher OGTT glucose levels when compared with the lean controls, suggesting that when metabolic stress was introduced, glucoregulation was similarly achieved in conditions of normal and reduced GIP production. At the same time, the circulating insulin levels were lower in GIP-lacking and GIP-reduced mice than those of WT mice on HFD, accompanied by decreased insulin resistance (Fig. 5*B* and Table 1). These data are in line with those of a previous study (36) examining the role of insulin in obesity and showing that, on an obese background, the reduction of insulin does not necessarily cause severe disturbance in blood glucose levels. The origins of the reduced insulin secretion are associated not only with reduced GIP signaling in β-cells, but also with changes in their area as well. Although GIP-reduced mice had a β-cell area similar to their WT counterparts on HFD, GIP-lacking mice had clearly fewer β-cells. Furthermore, in vitro islet studies found that the responsiveness of β-cells to glucose in GIP-reduced mice was similar to that in WT mice on HFD and was higher than that of the control mice. On the other hand, GIP-lacking mice had reduced insulin response to glucose, suggesting that reduction of GIP secretion might affect the ability of β-cells to respond adequately to GIP, but not as profoundly as in cases of complete absence of GIP secretion or GIPR signaling. Measurement of GIPR mRNA levels in the islets revealed similar values in WT and GIP-reduced mice, while GIP-lacking mice exhibited decreased expression of GIPR mRNA. GIPR mRNA expression levels in the adipose tissue did not show changes in WT and GIP-reduced mice, but, interestingly, they were increased in GIP-lacking mice, which is inconsistent with the islet data. Although previous studies have extensively addressed disruption of GIPR signaling, our GIP-lacking mice show for the first time a condition of complete lack of GIP secretion from intact K cells and might be useful in further studies.

We have investigated the mechanism of regulation of glucose homeostasis and reduced obesity in GIP-GFP KI on HFD. Previously, we reported an increase in fat oxidation and energy expenditure in GIPRKO mice fed HFD for a short period (37) and in GIPRKO mice with diminished insulin signaling (insulin receptor substrate 1 KO/GIPRKO mice) (38), indicating that increased fat oxidation accounts for the reduction of obesity in the absence of GIPR signaling. The current study has demonstrated increased fat oxidation in GIP-reduced mice, and, even more intensely, in GIP-lacking mice. This phenomenon might occur because of increased adiponectin levels via peroxisome proliferator–activated receptor α levels in the adipose tissue (37) or because of increased activity of the enzymes involved in β-oxidation in the liver, such as cluster of differentiation 36 and mitochondrial uncoupling protein 2 (38). GIP-lacking and GIP-reduced mice also exhibited higher energy expenditure while on an HFD. There are reports showing that increased energy expenditure is coupled with increased locomotor activity; disruption of GIPR signaling increases the activity of mice not only under HFD conditions, as in mice treated with GIPR antagonist (14) and GIPRKO mice (12), but also leads to increased spontaneous activity even during standard diet feeding, as described in double incretin receptor KO mice (29) and in adult or aged GIPRKO mice (39,40). Consistent with these data, GIP-lacking and GIP-reduced mice also exhibited a tendency toward increased activity, especially in the dark phase, although without a statistically significant difference.

In conclusion, our data suggest that the reduction of GIP secretion in vivo confirms the potent role of GIP in insulin secretion and leads to reduced obesity and reduced insulin resistance in HFD conditions without severely impairing glucose homeostasis and without disrupting the role of GIP in bone formation. These findings are potentially promising for a new therapeutic approach to obesity and type 2 diabetes.

Acknowledgments. The authors thank Shoichi Asano and Dr. Xibao Liu from the Department of Diabetes, Endocrinology and Nutrition, Graduate School of Medicine, Kyoto University, for their technical support regarding the study.

Funding. This study was supported by Scientific Research Grants from the Ministry of Education, Culture, Sports, Science, and Technology, Japan, and from the Ministry of Health, Labor, and Welfare, Japan.

Duality of Interest. N.I. served as a medical advisor for Takeda, Taisho Pharmaceutical, GlaxoSmithKline, Mitsubishi Tanabe Pharma; lectured for Meso Scale Discovery, Sanofi, Novartis Pharma, Dainippon Sumitomo Pharma, Kyowa Kirin, and Mitsubishi Tanabe Pharma; and received payment for his services. N.I.

received a clinical commission/joint research grant from Meso Scale Discovery, Eli Lilly Japan, Shiratori Pharmaceutical, Roche Diagnostics, and the Japan Diabetes Foundation; and also received a scholarship grant from Meso Scale Discovery, Japan Tobacco Inc., Nippon Boehringer Ingelheim, Takeda, Dainippon Sumitomo Pharma, Astellas Pharma, Daiichi-Sankyo, and Mitsubishi Tanabe Pharma. No other potential conflicts of interest relevant to this article were reported.

Author Contributions. D.N. researched the data; contributed to the discussion; and wrote, reviewed, and edited the manuscript. N.H. and N.I. contributed to the discussion, and reviewed and edited the manuscript. K.Su., S.Y., A.H., E.J., K.I., K.Sh., and T.H. contributed to the discussion. N.I. is the guarantor of this work and, as such, had full access to all the data in the study and takes responsibility for the integrity of the data and the accuracy of the data analysis.

Prior Presentation. Parts of the study were presented in abstract form at the 47th Annual Meeting of the European Association for the Study of Diabetes, Lisbon, Portugal, 12–16 September 2011; at the 48th Annual Meeting of the European Association for the Study of Diabetes, Berlin, Germany, 1–5 October 2012; and at the 73rd Scientific Sessions of the American Diabetes Association, Chicago, IL, 21–25 June 2013.

References

1. Krarup T, Holst JJ, Larsen KL. Responses and molecular heterogeneity of IR-GIP after intraduodenal glucose and fat. Am J Physiol 1985;249:E195–E200
2. Flatt PR. Dorothy Hodgkin Lecture 2008. Gastric inhibitory polypeptide (GIP) revisited: a new therapeutic target for obesity-diabetes? Diabet Med 2008;25:759–764
3. Baggio LL, Drucker DJ. Biology of incretins: GLP-1 and GIP. Gastroenterology 2007;132:2131–2157
4. Pederson RA, Brown JC. Inhibition of histamine-, pentagastrin-, and insulin-stimulated canine gastric secretion by pure "gastric inhibitory polypeptide". Gastroenterology 1972;62:393–400
5. Dupre J, Ross SA, Watson D, Brown JC. Stimulation of insulin secretion by gastric inhibitory polypeptide in man. J Clin Endocrinol Metab 1973;37:826–828
6. Yamada Y, Miyawaki K, Tsukiyama K, Harada N, Yamada C, Seino Y. Pancreatic and extrapancreatic effects of gastric inhibitory polypeptide. Diabetes 2006;55(Suppl. 2):S86–S91
7. Miyawaki K, Yamada Y, Yano H, et al. Glucose intolerance caused by a defect in the entero-insular axis: a study in gastric inhibitory polypeptide receptor knockout mice. Proc Natl Acad Sci U S A 1999;96:14843–14847
8. Herbach N, Bergmayr M, Göke B, Wolf E, Wanke R. Postnatal development of numbers and mean sizes of pancreatic islets and beta-cells in healthy mice and GIPR(^{dn}) transgenic diabetic mice. PLoS One 2011;6:e22814
9. Renner S, Fehlings C, Herbach N, et al. Glucose intolerance and reduced proliferation of pancreatic β-cells in transgenic pigs with impaired glucose-dependent insulinotropic polypeptide function. Diabetes 2010;59:1228–1238
10. Kim SJ, Winter K, Nian C, Tsuneoka M, Koda Y, McIntosh CH. Glucose-dependent insulinotropic polypeptide (GIP) stimulation of pancreatic β-cell survival is dependent upon phosphatidylinositol 3-kinase (PI3K)/protein kinase B (PKB) signaling, inactivation of the forkhead transcription factor Foxo1, and down-regulation of bax expression. J Biol Chem 2005;280:22297–22307
11. Widenmaier SB, Kim SJ, Yang GK, et al. A GIP receptor agonist exhibits β-cell anti-apoptotic actions in rat models of diabetes resulting in improved β-cell function and glycemic control. PLoS One 2010;5:e9590
12. Miyawaki K, Yamada Y, Ban N, et al. Inhibition of gastric inhibitory polypeptide signaling prevents obesity. Nat Med 2002;8:738–742
13. Tsukiyama K, Yamada Y, Yamada C, et al. Gastric inhibitory polypeptide as an endogenous factor promoting new bone formation after food ingestion. Mol Endocrinol 2006;20:1644–1651
14. McClean PL, Irwin N, Cassidy RS, Holst JJ, Gault VA, Flatt PR. GIP receptor antagonism reverses obesity, insulin resistance, and associated metabolic disturbances induced in mice by prolonged consumption of high-fat diet. Am J Physiol Endocrinol Metab 2007;293:E1746–E1755
15. Suzuki K, Harada N, Yamane S, et al. Transcriptional regulatory factor X6 (Rfx6) increases gastric inhibitory polypeptide (GIP) expression in enteroendocrine K-cells and is involved in GIP hypersecretion in high fat diet-induced obesity. J Biol Chem 2013;288:1929–1938
16. Preitner F, Ibberson M, Franklin I, et al. Gluco-incretins control insulin secretion at multiple levels as revealed in mice lacking GLP-1 and GIP receptors. J Clin Invest 2004;113:635–645
17. Yamane S, Harada N, Hamasaki A, et al. Effects of glucose and meal ingestion on incretin secretion in Japanese subjects with normal glucose tolerance. J Diabetes Invest 2012;3:80–85
18. Vollmer K, Holst JJ, Baller B, et al. Predictors of incretin concentrations in subjects with normal, impaired, and diabetic glucose tolerance. Diabetes 2008;57:678–687
19. Althage MC, Ford EL, Wang S, Tso P, Polonsky KS, Wice BM. Targeted ablation of glucose-dependent insulinotropic polypeptide-producing cells in transgenic mice reduces obesity and insulin resistance induced by a high fat diet. J Biol Chem 2008;283:18365–18376
20. Fujita Y, Chui JWY, King DS, et al. Pax6 and Pdx1 are required for production of glucose-dependent insulinotropic polypeptide in proglucagon-expressing L cells. Am J Physiol Endocrinol Metab 2008;295:E648–E657
21. Parker HE, Habib AM, Rogers GJ, Gribble FM, Reimann F. Nutrient-dependent secretion of glucose-dependent insulinotropic polypeptide from primary murine K cells. Diabetologia 2009;52:289–298
22. Habib AM, Richards P, Cairns LS, et al. Overlap of endocrine hormone expression in the mouse intestine revealed by transcriptional profiling and flow cytometry. Endocrinology 2012;153:3054–3065
23. Brubaker PL. Regulation of intestinal proglucagon-derived peptide secretion by intestinal regulatory peptides. Endocrinology 1991;128:3175–3182
24. Roberge JN, Brubaker PL. Regulation of intestinal proglucagon-derived peptide secretion by glucose-dependent insulinotropic peptide in a novel enteroendocrine loop. Endocrinology 1993;133:233–240
25. Pacheco-Pantoja EL, Ranganath LR, Gallager JA, Wilson PJM, Fraser WD. Receptors and effects of gut hormones in three osteoblastic cell lines. BMC Physiol 2011;11:12
26. Zhong Q, Itokawa T, Sridhar S, et al. Effects of glucose-dependent insulinotropic peptide on osteoclast function. Am J Physiol Endocrinol Metab 2007;292:E543–E548
27. Kieffer TJ. GIP or not GIP? That is the question. Trends Pharmacol Sci 2003;24:110–112
28. Creutzfeldt W, Ebert R, Willms B, Frerichs H, Brown JC. Gastric inhibitory polypeptide (GIP) and insulin in obesity: increased response to stimulation and defective feedback control of serum levels. Diabetologia 1978;14:15–24
29. Hansotia T, Maida A, Flock G, et al. Extrapancreatic incretin receptors modulate glucose homeostasis, body weight, and energy expenditure. J Clin Invest 2007;117:143–152
30. Harada N, Yamada Y, Tsukiyama K, et al. A novel GIP receptor splice variant influences GIP sensitivity of pancreatic beta-cells in obese mice. Am J Physiol Endocrinol Metab 2008;294:E61–E68
31. Harada N, Hamasaki A, Yamane S, et al. Plasma gastric inhibitory polypeptide and glucagon-like peptide-1 levels after glucose loading are associated with different factors in Japanese subjects. J Diabetes Invest 2011;2:193–199
32. Seino Y, Yabe D. Glucose-dependent insulinotropic polypeptide and glucagon-like peptide-1: incretin actions beyond the pancreas. J Diabetes Invest 2013;4:108–130
33. Knapper JME, Puddicombe SM, Morgan LM, Fletcher JM. Investigations into the actions of glucose-dependent insulinotropic polypeptide and glucagon-like peptide-1(7-36)amide on lipoprotein lipase activity in explants of rat adipose tissue. J Nutr 1995;125:183–188
34. Song DH, Getty-Kaushik L, Tseng E, Simon J, Corkey BE, Wolfe MM. Glucose-dependent insulinotropic polypeptide enhances adipocyte development and glucose uptake in part through Akt activation. Gastroenterology 2007;133:1796–1805

35. Parkin SM, Walker K, Ashby P, Robinson DS. Effects of glucose and insulin on the activation of lipoprotin lipase and on protein-synthesis in rat adipose tissue. Biochem J 1980;188:193–199
36. Mehran AE, Templeman NM, Brigidi GS, et al. Hyperinsulinemia drives diet-induced obesity independently of brain insulin production. Cell Metab 2012;16: 723–737
37. Naitoh R, Miyawaki K, Harada N, et al. Inhibition of GIP signaling modulates adiponectin levels under high-fat diet in mice. Biochem Biophys Res Commun 2008;376:21–25
38. Zhou H, Yamada Y, Tsukiyama K, et al. Gastric inhibitory polypeptide modulates adiposity and fat oxidation under diminished insulin action. Biochem Biophys Res Commun 2005;335:937–942
39. Faivre E, Gault VA, Thorens B, Hölscher C. Glucose-dependent insulinotropic polypeptide receptor knockout mice are impaired in learning, synaptic plasticity, and neurogenesis. J Neurophysiol 2011;105:1574–1580
40. Yamada C, Yamada Y, Tsukiyama K, et al. Genetic inactivation of GIP signaling reverses aging-associated insulin resistance through body composition changes. Biochem Biophys Res Commun 2007;364:175–180